THE JOURNAL OF BIOLOGICAL CHEMISTRY Vol. 275, No. 10, Issue of March 10, pp. 6945–6955, 2000
Printed in U.S.A.

SPACRCAN, a Novel Human Interphotoreceptor Matrix Hyaluronan-binding Proteoglycan Synthesized by Photoreceptors and Pinealocytes*

(Received for publication, August 9, 1999, and in revised form, December 3, 1999)

Shreeta Acharya‡§¶, Victoria C. Foletta§‖, Jung Wha Lee, Mary E. Rayborn‡, Ignacio R. Rodriguez**, W. Scott Young III‖, and Joe G. Hollyfield‡ ‡‡**

*From the ‡Cole Eye Institute, The Cleveland Clinic Foundation, Cleveland, Ohio 44195, ‖The National Institute of Mental Health, and **The National Eye Institute, The National Institutes of Health, Bethesda, Maryland 20892*

The interphotoreceptor matrix is a unique extracellular complex occupying the interface between photoreceptors and the retinal pigment epithelium in the fundus of the eye. Because of the putative supportive role in photoreceptor maintenance, it is likely that constituent molecules play key roles in photoreceptor function and may be targets for inherited retinal disease. In this study we identify and characterize SPACRCAN, a novel chondroitin proteoglycan in this matrix. SPACRCAN was cloned from a human retinal cDNA library and the gene localized to chromosome 3q11.2. Analysis of SPACRCAN mRNA and protein revealed that SPACRCAN is expressed exclusively by photoreceptors and pinealocytes. SPACRCAN synthesized by photoreceptors is localized to the interphotoreceptor matrix where it surrounds both rods and cones. The functional protein contains 1160 amino acids with a large central mucin domain, three consensus sites for glycosaminoglycan attachment, two epidermal growth factor-like repeats, a putative hyaluronan-binding motif, and a potential transmembrane domain near the C-terminal. Lectin and Western blotting indicate an M_r around 400,000 before and 230,000 after chondroitinase ABC digestion. Removal of *N*- and *O*-linked oligosaccharides reduces the M_r to approximately 160,000, suggesting that approximately 60% of the mass of SPACRCAN is carbohydrate. Finally, we demonstrate that SPACRCAN binds hyaluronan and propose that associations between SPACRCAN and hyaluronan may be involved in organization of the insoluble interphotoreceptor matrix, particularly as SPACRCAN is the major proteoglycan present in this matrix.

The light-sensitive photoreceptor inner and outer segments project from the outer retinal surface into a carbohydrate-rich IPM[1] (1). Several structure-function activities of fundamental importance to vision are thought to be mediated by the IPM, including visual pigment chromophore exchange, metabolite trafficking, retinal adhesion, photoreceptor alignment, and photoreceptor membrane turnover (2–12). Because this matrix resides in such a key location and is putatively crucial in supporting photoreceptor function, additional information is required as to the identity, role, and involvement of specific IPM molecules in mediating these activities.

Early attempts to remove IPM components for subsequent characterization used saline rinses of the outer retinal surface, which succeeded in isolating some soluble molecules. For example, the interphotoreceptor matrix retinoid-binding protein was first isolated from the IPM by rinsing, which also removed a variety of enzymes, some mucins, and immunoglobulins (13–17). The retention of other less soluble molecules following aqueous rinses was not initially appreciated but was clearly documented in the studies of the IPM in *Xenopus* (18) and rat (19).

Recently, an abundant sialoglycoprotein that is retained in the human IPM following rinsing was characterized and named SPACR (20). A polyclonal antibody prepared against SPACR intensely labels the rod-associated matrix with weaker labeling of the cone matrix (20). Sequence analysis of peptides from purified SPACR revealed 100% identity to the deduced sequence of interphotoreceptor matrix proteoglycan 1 (GenBank™ accession number AF047492) cDNA (also called IPM150) (21). The gene product of interphotoreceptor matrix proteoglycan 1 is listed in GenBank™ as a chondroitin sulfate proteoglycan core protein, but our analysis indicates that it is a glycoprotein and not a proteoglycan (21).

Earlier reports document the presence of another prominent protein in the insoluble IPM. This molecule, initially referred to as IPM200 (8), is clearly a proteoglycan core protein because it will only enter a 7.5% polyacrylamide gel after digestion with chondroitinase ABC (23). Furthermore, it shows intense immunoreactivity in Western blots to a chondroitin ΔDi6S monoclonal antibody (23). Until now the identity of this proteoglycan has remained unknown. In this study we describe the cloning and characterization of the human cDNA encoding this novel proteoglycan in addition to the chromosomal localization of the gene counterpart. The identification of the proteoglycan came about during cloning attempts of the human homolog of PG10.2, a gene that is expressed specifically in rat pineal gland

* This work was supported by Grant EY 02362 from the National Institutes of Health, The Foundation Fighting Blindness, Hunt Valley, MD, The Retina Research Foundation, Houston, TX, and funds from The Cleveland Clinic Foundation.

The nucleotide sequence(s) reported in this paper has been submitted to the GenBank™/EBI Data Bank with accession number(s) AF157624.

§ Contributed equally to this analysis.

¶ Recipient of an award from the Knights Templar Eye Foundation, Chicago, Il.

‡‡ Recipient of the 1999 Ocular Cell and Molecular Biology Prize from Allergan Laboratory for career contributions to vision research. To whom correspondence should be addressed. Tel.: 216-445-3252; Fax: 216-445-3670.

[1] The abbreviations used are: IPM, interphotoreceptor matrix; SPACR, sialoprotein associated with cones and rods; ABC, avidin-biotin-peroxidase complex; ΔDi6S, chondroitin-6-sulfate Δdisaccharide; PNA, peanut agglutinin; HA, hyaluronan; PCR, polymerase chain reaction; PBS, phosphate-buffered saline; PAGE, polyacrylamide gel electrophoresis; BSA, bovine serum albumin; CPC, cetylpyridinium chloride; EFEMP-1, EGF fibrillin-like extracellular matrix protein-1; EGF, epidermal growth factor; GAG, glycosaminoglycan; Healon, the trade name for highly purified HA used in ophthalmic surgery; Nonidet P-40, nonylpenoxyethanol; PG10.2, rat pineal gland clone 10.2.

and retina (24). The N-terminal sequence of the proteoglycan core protein isolated from the human IPM matched the deduced amino acid sequence of the human PG10.2 homolog. We named this gene and its product "SPACRCAN," because it is a novel proteoglycan located in the subretinal space, the term used by ophthalmologists for the IPM. We document the expression of the SPACRCAN gene in photoreceptors and pinealocytes and localize SPACRCAN in the IPM where it surrounds both rods and cones. SPACRCAN is retained in the insoluble IPM through its binding to hyaluronan, suggesting that one function of SPACRCAN is to participate with the glycoprotein SPACR in binding and organizing hyaluronan into the primary scaffold of the insoluble IPM (25). Finally, there are homologous regions between the deduced amino acid sequences of human SPACRCAN and the glycoprotein SPACR, which suggests a novel family of IPM-specific molecules.

EXPERIMENTAL PROCEDURES

Reagents—Avidin-conjugated lectins wheat germ agglutinin and PNA, biotinylated horseradish peroxidase, streptavidin, and goat anti-rabbit IgG were obtained from Vector Laboratories (Burlingame, CA). Nitro blue tetrazolium, 5-bromo-4-chloro-3-indolyl phosphate tablets, iodoacetic acid, and dithiothreitol were purchased from Sigma. Protease inhibitors were from Roche Molecular Biochemicals, (Indianapolis, IN). 3,3′-Diaminobenzidine tablets were from Amresco (Solon, OH). The biotinylated monoclonal antibody prepared against chondroitinase ABC-digested proteoglycan and chondroitin ΔDi6S (from clone 3-B-3) were from Seikagaku Corporation (Ijamsville, MD). Chondroitinase ABC (protease free) and *Streptomyces* hyaluronidase were also from Seikagaku Corporation (Ijamsville, MD). *N*- and *O*-glycosidases were from Oxford GlycoSciences, (Wakefield, MA). Cetylpyridinium chloride was obtained from ICN Biomedicals, (Aurora, OH). Immobilon-P membranes were purchased from Millipore, (Bedford, MA). Healon, Amersham Pharmacia Biotech, was the source of HA. Gel Code stain was obtained from Pierce. The 22-mer HA oligosaccharides were a gift from Markku Tammi and have been described in previous work (see Ref. 26).

Tissue Sources—The 42 human eyes used in this analysis were obtained from the Cleveland Eye Bank, Cleveland, OH. Donor ages ranged from 14 to 77 years, with postmortem times between 2 and 12 h. Seven human pineal glands with donor ages from 20 to 78 years were also used; five were obtained through the Cooperative Human Tissue Network at The Cleveland Clinic Foundation, Department of Anatomic Pathology, and two were from the section of Neuropathology, Clinical Brain Disorders Branch, NIMH, Bethesda, MD.

cDNA Library Screen—Approximately 1×10^6 bacteriophage clones from a λgt10 human retinal cDNA library (kindly provided by Dr. Jeremy Nathans, Johns Hopkins University School of Medicine, Baltimore, MD) were screened (27) using a rat PG10.2 cDNA probe. The cDNA probe was derived by PCR using rat PG10.2 sequence-specific forward (5′-TGGTTTTGGCCCAAATGATTATGTTTCTCC) and reverse (5′-CCCAGGGTGGCATTTGCACTTTGC) primers and the rat PG10.2 cDNA as the DNA template (24). The PCR product was purified using QIAquick gel extraction kit (QIAGEN, Valencia, CA) and random primer labeled with [α-^{32}P]dCTP (3000 Ci/mmol, ICN Biomedicals, Aurora, OH) and the Prime-It II kit (Stratagene, La Jolla, CA) according to the manufacturer's instructions. The nitrocellulose membrane filters (Schleicher & Schuell) were prehybridized for 3 h in 5× Denhardt's solution (0.1% Ficoll, type 400, 0.1% polyvinylpyrrolidone, 0.1% bovine serum albumin, fraction V) and 3× SSPE (1× = 0.15 M NaCl/0.01 M NaH_2PO_4. H_2O, pH 7.4) at 60 °C. Hybridization was performed overnight in 1× Denhardt's, 3× SSPE, and 10^6 cpm/ml of the rat PG10.2 PCR probe at 60 °C. Filters were washed for 15 min, five times, in 0.2× SSPE and 0.2% SDS at 60 °C and exposed to Kodak XAR film for 1–2 days at −80 °C.

Reverse Transcriptase PCR and PCR Amplification—One microgram of DNase I-treated total RNA extracted from human retinal tissue was used as the template for each first strand cDNA synthesis. To generate the central cDNA region of human SPACRCAN, the reverse primer, 5′-CCTCTAGCAGGGTGGAGATTGTGG, designed from the cDNA sequence of the phage clone, hPG10.2.3, was used to synthesize the first strand cDNA. Amplification of the cDNA was performed with forward (5′-CTCTGGTCAGAAAGTCCTTTG) and reverse (5′-CAGTAGAGGCAGAGATTGCTACAG) primers designed from human SPACRCAN genomic sequence data[2] and from the hPG10.2.3 cDNA sequence, respectively. The 5′-cDNA region of SPACRCAN was generated using the reverse primer (5′-CAGTAGAGGCAGAGATTGCTACAG) for first strand cDNA synthesis. The cDNA amplification was performed using low stringency PCR conditions with the forward (5′-TGGTTTTGGCCCAAATGATTATGTTTCTCC) and reverse (5′-GTCCTTTCCTCAGAAGCCACAG) primers that were derived from rat PG10.2 cDNA sequence and from human SPACRCAN cDNA sequence, respectively. Low stringency PCR was performed at the following temperatures after an initial incubation of 94 °C for 3 min, 94 °C for 30 s, 45 °C for 30 s, and 68 °C for 2 min for two preliminary cycles. For the next 30 cycles, the conditions were as follows: 94 °C for 30 s, 50 °C for 30 s, and 72 °C for 2 min with a final 10-min extension step at 72 °C. All other PCR procedures were performed as follows: 94 °C for 30 s, 55 °C for 30 s, and 72 °C for 3.5 min for 30 cycles after an initial incubation at 94 °C for 3 min and with a final 10-min extension step at 72 °C. The first strand cDNA syntheses and PCR steps were performed using Superscript II RNase H-reverse transcriptase and Platinum *Taq* DNA polymerase (Life Technologies, Inc.), respectively, as recommended by the manufacturer.

DNA Sequencing and Analysis—Sequencing was performed by the dideoxynucleotide chain termination DNA-sequencing method using the T7 Sequenase version 2.0 DNA sequencing kit (Amersham Pharmacia Biotech). Sequence was analyzed using DNA Strider 1.2 (Christian Marck, Center d'Etudes de Saclay, Cedex, France) and GeneWorks (Intelligenetics, Mountain View, CA) software.

Chromosomal Localization—The forward (5′-CTCACATGACAGTTAGATGG) and reverse (5′-CAGAGTCTCTGTGACCTACAG) PCR primers used for chromosomal localization of the SPACRCAN gene were designed from the 3′-untranslated region of SPACRCAN, identified in image clone AA815118 from a BLAST search using the rat PG10.2 sequence. Localization was performed by Research Genetics, Inc., using DNA from each of 93 radiation hybrid panel cell lines as PCR templates. The localization was confirmed by fluorescent *in situ* hybridization analysis (Genome Systems, Inc, St. Louis, MO).

Northern Analysis—Total RNA from human tissues was either purchased from CLONTECH (Palo Alto, CA) or isolated from the human tissues using RNAeasy kit (QIAGEN Inc., Valencia, CA). Macula and peripheral retina RNA were isolated from 5-mm punches from fresh monkey retina as described previously (28). The RNA was separated by electrophoresis in a 1.2% agarose formaldehyde gel at 56 V for 3.5 h. The gel was stained with SYB green II (Molecular Probes, Eugene, OR) then scanned using a STORM 860 apparatus (Molecular Dynamics, Inc., Sunnyvale, CA). The gel was blotted and probed with a 462-base pair SPACRCAN probe generated by PCR using the forward (5′-CCGTGTATGAAAGTCACAGG) and reverse (5′-CACAGCATTCAGTCTTTATAG) primers. The quantification was performed using Molecular Dynamic's ImageQuant 5.0 software and Microsoft (Seattle, WA) Excel software using a similar method (29).

In Situ Hybridization—The cDNA insert of the phage clone, hPG10.2.3, was subcloned into the *Eco*RI site of the pGEM-4Z vector (Promega, Madison, WI). Sense and antisense riboprobes, labeled with ^{35}S-labeled UTP (1250 Ci/mmol, NEN Life Science Products), were generated using SP6 and T7 RNA polymerases, respectively. *In situ* hybridization histochemistry was performed on fresh frozen human retinal and pineal gland sections cut at 12 μm. These sections were processed as described previously (30) and were dipped in emulsion and developed after exposure for 2 months. Sections were examined with bright and darkfield illumination using a Leitz photomicroscope. Images were digitized using a SenSys-KF1401E CCD camera (Photometrics, Tuscon, AZ) and manipulated with IPLab (Scanalytics, Fairfax, VA), Adobe 5.0 (Adobe Systems, San Jose, CA), and Canvas 6 (Deneba, Miami, FL) software on a PowerPC Macintosh computer.

IPM Isolation—After bisecting the eye, retinas were removed from the posterior pole and washed extensively with PBS containing protease inhibitors to remove soluble molecules followed by detachment of the insoluble IPM with distilled water (21, 31). The insoluble IPM was collected (20) after centrifugation, and the pellet was solubilized in 0.1 M Tris-buffered saline, pH 8.0, containing 5 mM dithiothreitol.

Enzyme Digestions—Chondroitinase ABC: 50 μl of 1 mg/ml IPM extract was resuspended in 0.1 M Tris acetate buffer, pH 7.3, and 3 milliunits of the enzyme, containing protease inhibitors, was added to the tube. The reaction was allowed to proceed at 37 °C for 3 h. *Streptomyces* hyaluronidase: IPM extract (100 μg of total protein) was incubated in 50 mM sodium acetate buffer, pH 6.0, for 2 h at 37 °C with *Streptomyces* hyaluronidase (2–5 TRU). *N*-Glycosidase: Samples (50 μg)

[2] V. C. Foletta, unpublished data.

were denatured in 0.05 M phosphate buffer containing 0.2% SDS and 50 mM dithiothreitol at 100 °C for 5 min. Nonidet P-40 was added to a final concentration of 0.7% in 100 μl of sample volume to which was added 0.3 milliunits in 1 μl of recombinant peptide *N*-glycosidase F. The digestion was continued overnight at 37 °C. Neuraminidase: 50 μg of total protein was dissolved in 100 μl of 0.1 M sodium phosphate buffer, pH 6.5. 50 milliunits/μl neuraminidase were added followed by incubation for 1 h at 37 °C. *O*-Glycosidase: IPM sample (50 μg), predigested with neuraminidase as described above, was denatured by boiling in 0.1% SDS, 10 mM sodium cacodylate buffer, pH 6.0. Nonidet P-40 was added in 10-fold excess of SDS by weight followed by 50 milliunits of *O*-glycosidase and overnight incubation at 37 °C.

Antibody Production—The insoluble IPM removed with distilled water was isolated as described previously (31). The IPM pellet was obtained by centrifugation at 400 × *g* for 15 min on a table top centrifuge. The pellet was resuspended in cold 0.1 M Tris-buffered saline (pH 8.0 containing 5 mM dithiothreitol). The supernatant was collected after centrifugation (12,000 rpm) in a refrigerated microfuge. The supernatant was diluted 2× with 0.1 M NaOAc, pH 6.0, and digested with chondroitinase ABC (300 milliunits/ml) for 3 h at 37 °C. At the end of the incubation, an equal volume of SDS sample buffer was added to the IPM extract, the sample was denatured by boiling for 5 min in the presence of 5% 2-mercaptoethanol, and the proteins were separated on 7.5% SDS-PAGE (30 μg of total protein/lane). After electrophoresis the gel was rinsed with water three times before staining with Gel Code Blue. The gels were destained with water, and the 230-kDa bands were removed, minced, and sent to Biodesign Inc., Kennebunk, Maine for immunization in rabbits. Approximately 200 μg of SPACRCAN was injected/boost. Antibodies to SPACRCAN reached a suitable titer for use in Western blotting and immunocytochemical studies following the third boost.

Western Blotting—Sample extracts were subjected to SDS-PAGE and electroblotted onto Immobilon-P membranes followed by incubation in PBS containing 2% BSA at pH 7.5 for 30 min. BSA was replaced by the biotinylated lectin (20 μg/ml) in 1% BSA-PBS for lectin blots and incubated for 3 h at room temperature. For Western blots, the membranes were incubated with anti-SPACRCAN (1:1000) or anti-ΔDi6S (1:100) in PBS-BSA overnight at 4 °C after BSA blocking. The membranes were washed with PBS-Tween (3 times) and incubated with biotinylated horseradish peroxidase-Avidin complex or alkaline phosphatase-conjugated secondary antibody (1:5000) for 1 h at room temperature. The membranes were washed and the color reaction developed using the substrates 5-bromo-4-chloro-3-indolyl phosphate-nitro blue tetrazolium or 3,3′-diaminobenzidine.

PNA-Agarose Affinity Chromatography—IPM extract as prepared above was digested with chondroitinase ABC (3 milliunits/50 μg of protein) in 50 mM Tris acetate buffer, pH 7.3, at 37 °C for 2 h. This was loaded on a PNA-agarose affinity resin (Vector labs) prequilibrated with PBS. The column was washed with PBS and eluted with 0.2 M lactose. Fractions were dialyzed and then analyzed by SDS-PAGE followed by Gel Code Blue staining for the presence of SPACRCAN.

Protein/Peptide Sequencing—IPM extracts in Tris-HCl were further separated on a 7.5% SDS-PAGE gel. The gel was stained with Gel Code Blue, and the band excised, destained, and sent to the Howard Hughes Medical Institute Biopolymer Laboratory and WM Keck Foundation Biotechnology Resource Foundation at Yale University, New Haven, CT for digestion with trypsin and separation by liquid chromatography-mass spectrometry. Three of the resultant peptides were sequenced by Edman degradation. Affinity purified SPACRCAN was separated by SDS-PAGE and transferred to Immobilon-P membranes, stained with Coomassie Blue. SPACRCAN bands were excised and sequenced on an Applied Biosystems Gas phase sequencer at the Case Western Biotechnology Core Laboratory, Cleveland, Ohio.

CPC Precipitation—To demonstrate HA binding to SPACRCAN we used a protocol similar to that described (21). Briefly, PNA-agarose-purified SPACRCAN core protein samples (1 μg) in 50 mM Tris acetate buffer (pH 7.3) containing 0.5 M NaCl were incubated for 1 h at room temperature with and without Healon (50 μg). Control samples were digested with *Streptomyces* hyaluronidase (1 TRU) for 1 h at 37 °C prior to CPC precipitation. Inhibition of endogenous HA binding was performed in the presence of HA oligosaccharides (100 μg/ml). BSA (2 μg) incubated with Healon was used as a negative control. CPC (1.25% final concentration) was added to the samples and further incubated for 1 h. The CPC pellet and supernatant were obtained by centrifugation (12,000 rpm) of the sample for 15 min at room temperature. The pellets were rinsed twice with 1% CPC in Tris acetate buffer. Pellets were resuspended in 20 μl of water and boiled in SDS-PAGE sample buffer (32) before the proteins in the pellet and supernatant were separated by PAGE. After electrophoresis the proteins were transferred to polyvinylidene difluoride membranes using the Bio-Rad semi-dry blotting system. The membranes were blocked using 2% BSA in PBS before incubating with 1:100 dilution of biotinylated ΔDi6S antibody overnight at 4 °C. After incubation with avidin-conjugated horseradish peroxidase (1:5000 in PBS), the protein bands were visualized with the peroxidase color reaction as described previously. BSA was included in the CPC precipitation studies as a negative control (21).

Immunocytochemistry—Eyes arrived at the laboratory in eye bank jars on ice. They were gently opened with a razor blade, cutting posterior to the limbus prior to immersion fixation. Freshly isolated eyes and pineal glands used for anti-SPACRCAN immunocytochemistry were preserved in a fixative containing 4% formaldehyde (freshly prepared from paraformaldehyde), in 0.1 M phosphate buffer (pH 7.2). After removal from the fixative, tissues were rinsed in 3 × 10 min changes of 0.1 M phosphate buffer and processed for paraffin microscopy using standard dehydration and infiltration procedures. Tissue sections cut at 7 μm were placed on Superfrost slides, deparaffinized with xylene, and hydrated through graded ethanols prior to enzyme digestion or antibody application.

Chondroitinase ABC digestions were performed on deparaffinized tissue sections mounted on microscope slides (Seikagaku Corp., 460 milliunits/ml in 0.1 M Tris acetate, pH 7.3, 37 °C, 1 h). Tissue sections were incubated with 6% BSA in phosphate buffer (0.1 M, pH 7.2) for 30 min to block nonspecific antibody binding. Sections were incubated with the primary SPACRCAN antibody (diluted 1:2000) in 6% BSA, 0.1 M phosphate buffer overnight at 4 °C. After rinsing extensively with 0.1 M phosphate buffer, sections were treated with ABC (Vector Labs., 1:200 dilution) for 1 h at room temperature. Sections were washed with 0.1 M phosphate buffer and incubated in 0.05% 3,3′-diaminobenzidine (Sigma) and 0.03% hydrogen peroxide in the phosphate buffer at room temperature. Sections were examined unstained with transmitted light or Nomarski optics using a Zeiss Axiophot photomicroscope. Images were digitized using a Hamamatsu CCD camera and manipulated with Photoshop 4.0 software on a Power Macintosh computer.

RESULTS

Cloning of Human SPACRCAN cDNA—To clone the human SPACRCAN cDNA, phage clones of a human retina cDNA library were screened using a partial cDNA of the rat homolog, PG10.2 (24), as a probe. Six positive clones were isolated and the nucleotide sequence of the largest clone (hPG10.2.3, 1.95 kilobases) was determined. Comparison with the rat PG10.2 cDNA revealed that hPG10.2.3 contained the 3′-half of SPACRCAN′s open reading frame. The remaining SPACRCAN cDNA was obtained by employing reverse transcriptase-PCR using RNA extracted from human retina and by subsequent PCR amplification. The combined nucleotide sequence from the three partially overlapping cDNA clones contains 3989 base pairs (Fig. 1).

Two in-frame methionine codons (ATG) are present at nucleotides 15 and 21, and a stop codon (TAA) is evident at nucleotide 3738. At present it is unclear which AUG codon in SPACRCAN mRNA would be preferred for translation initiation of SPACRCAN mRNA. Usually initiation occurs from the first AUG according to the Kozak scanning model (33). However, the second AUG has an A, a purine, in position −3, which is normally critical for function (33). It is also possible that both codons are used.

Downstream to the stop codon at nucleotide 3962 is a consensus polyadenylation motif (AATAAA). If this is the true end of the 3′-untranslated region of SPACRCAN, then a large 5′-untranslated region is likely to exist as the SPACRCAN transcript is approximately 9.0 kilobases (Fig. 2). Finally, SPACRCAN has a 79% nucleotide sequence identity with rat PG10.2 (24), which strongly suggests that they are indeed orthologs.

Chromosomal Localization of SPACRCAN—The SPACRCAN gene was localized to chromosome 3q11.2 using radiation hybrid panel screening and confirmed by fluorescent *in situ* hybridization analysis. When the data were submitted to the

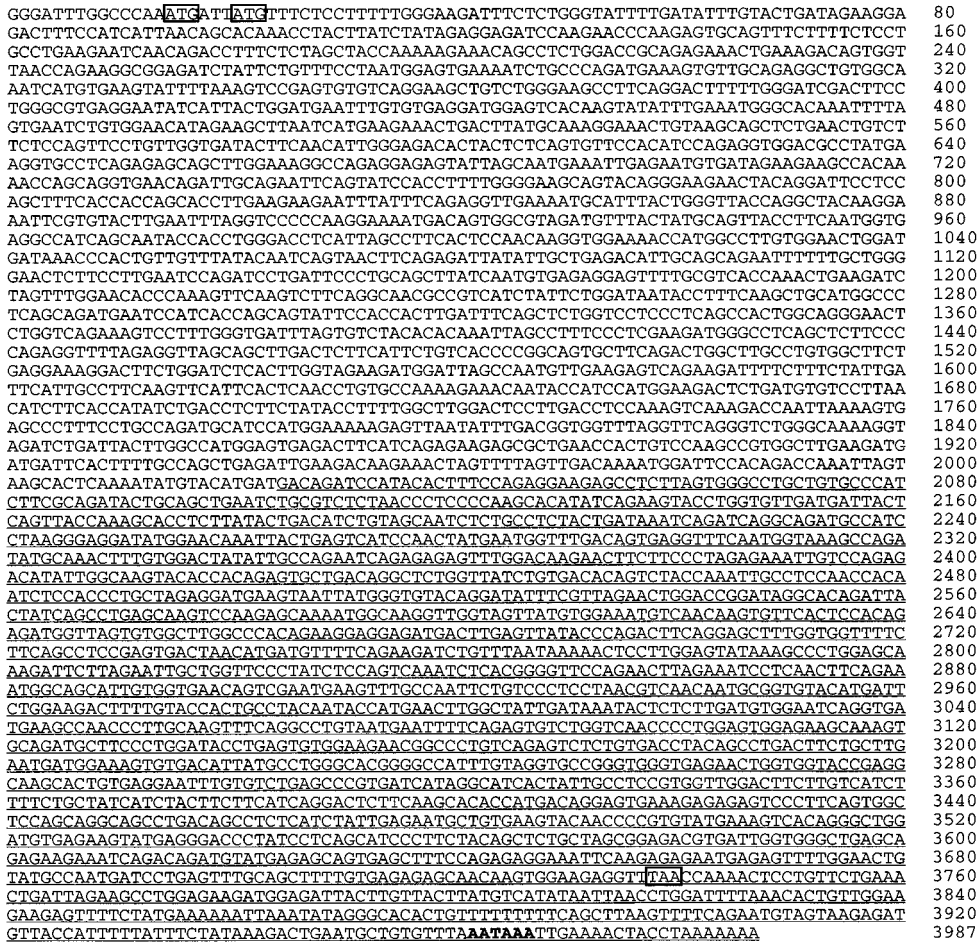

FIG. 1. **Nucleotide sequence of the SPACRCAN cDNA.** The 3989-base pair sequence was derived from partial cDNA clones obtained from a human retina cDNA library (*underlined*) and from reverse transcriptase-PCR and PCR products. The potential start and stop codons are *boxed* and the polyadenylation motif is highlighted in *bold*. The nucleotide sequence for the human SPACRCAN cDNA has been deposited in GenBank™/EBI/DDBJ data bases under GenBank™ Accession Number AF157624.

Whitehead/MIT server and tested against the current framework markers, SPACRCAN was localized between markers WI-11447 and WI-16656 (34).

Tissue Distribution of SPACRCAN Expression—Northern blot analysis on a variety of human tissues was performed to determine the tissue specificity and the relative levels of expression of SPACRCAN mRNA (Fig. 2). Approximately 5 μg of total RNA was used for each tissue. The blot was probed with a 3′-end SPACRCAN-specific cDNA probe. The relative levels of expression were determined by normalizing the SYB green II-stained 28 S ribosomal RNA band to the signal generated by the probe using a STORM 860 phosphoimager (29). The SPACRCAN hybridization signal was observed exclusively in the retina and pineal gland mRNA samples, indicating that the SPACRCAN gene is expressed only in these tissues. The predominant SPACRCAN mRNA appears to be approximately 9 kilobases in length although a smaller and more diffuse signal is also evident at approximately 4.4 kilobases (Fig. 2).

Cellular Localization of SPACRCAN Expression—In situ hybridization was performed on fresh frozen sections of the human retina and pineal gland. The ^{35}S-labeled antisense riboprobe signal was localized to the outer retina with a high density of silver grains over the photoreceptor inner segments and a weaker density over the photoreceptor nuclei (Fig. 3, *A* and *B*). Both rod and cone photoreceptors were labeled. Retinal sections incubated with the ^{35}S-labeled sense riboprobe were virtually free of silver grains (Fig. 3, *C* and *D*). In the pineal gland, SPACRCAN ^{35}S-labeled antisense hybridization was evident throughout most regions with the exception of the connective tissue septa. These septal areas also contain blood vessels, and gliotic or fibrotic-like inclusions (Fig. 3, *E*, *G,* and *H*). Pineal sections incubated with the ^{35}S-labeled sense riboprobe were virtually free of silver grains (Fig. 3*F*).

Features of the Putative Polypeptide—The nucleotide sequence of the SPACRCAN cDNA presented in Fig. 1 contains an open reading frame that encodes 1241 amino acids. The deduced amino acid of the SPACRCAN polypeptide is presented in Fig. 4. Several potentially important features are evident. (*a*) A large mucin-like domain, containing numerous potential *O*-linked glycosylation sites (76 serine and 35 threonine residues), is located in the central part of the sequence (Thr^{393}-Thr^{835}). (*b*). Six consensus sites for *N*-linked glycosylation are present in two clusters, four on the N-terminal side and two on the C-terminal side of the mucin domain (at residues Asn^{154}, Asn^{301}, Asn^{320}, Asn^{370}, Asn^{942}, and Asn^{956}). (*c*) Four consensus sites for GAG attachment are present. The first is at residue Ser^{603}, near the center of the mucin domain, which conforms to the consensus sequence SG*X*G (35). The other three are on the C-terminal side of the mucin domain (at residues Ser^{1007}, Ser^{1031}, and Ser^{1187}) and conform to the consensus sequence SG (acidic) (36). Ser^{1031} is located between two cysteine residues (Cys^{1025} and Cys^{1036}) and may not be functional. (*d*) A linear HA-binding motif is present in the deduced

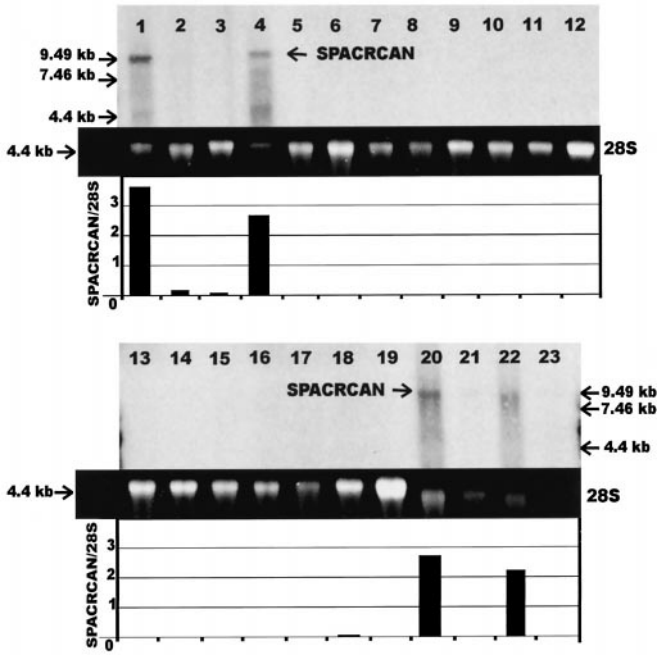

FIG. 2. **Multitissue Northern blot analysis of SPACRCAN performed on 19 human tissues (*lanes 1–19*) and 4 monkey eye tissues (*lanes 20–23*).** Each lane was loaded with 5 μg of total RNA and separated by agarose gel electrophoresis as described under "Experimental Procedures." The sample order is: *lane 1,* retina; *2,* pigment epithelium/choroid; *3,* brain; *4,* pineal gland; *5,* cerebellum; *6,* heart; *7,* skeletal muscle; *8,* liver; *9,* kidney; *10,* stomach; *11,* small intestine; *12,* lung; *13,* spleen; *14,* prostate; *15,* testis; *16,* placenta; *17,* uterus; *18,* fetal brain; *19,* fetal liver; *20,* neural macula; *21,* macular pigment epithelium/choroid; *22,* peripheral retina; and *23,* peripheral pigment epithelium/choroid. The graph shows the relative ratio of SPACRCAN to the 28S band as described under "Experimental Procedures." *kb*, kilobase.

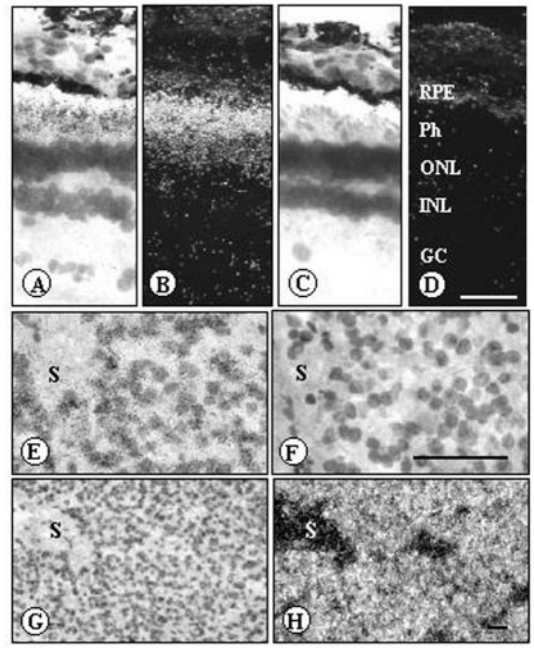

FIG. 3. ***In situ* hybridization histochemical localization of SPACRCAN expression in retina (*A–D*) and pineal gland (*E–H*).** Both brightfield (*A*, *E*, and *G*) and darkfield (*B* and *H*) photomicrographs demonstrate hybridization of SPACRCAN mRNA with an antisense ^{35}S-labeled dUTP riboprobe generated from hPG10.2.3 cDNA clone. No labeling is evident with the sense riboprobe (*C*, *D*, and *F*). *RPE*, retinal pigment epithelium; *Ph*, photoreceptor layer; *ONL*, outer nuclear layer; *INL*, inner nuclear layer; *GC*, ganglion cell layer; *S*, connective tissue septa. *Bar* in *A–D* and *E–H* represents 50 and 100 μm, respectively.

sequence spanning residues Arg^{1125}-Arg^{1133} (37).[3] (*e*) Two EGF-like motifs, arranged in tandem, are present near the C terminus (Cys^{1014}-Cys^{1050} and Cys^{1054}-Cys^{1092}). EGF-like motifs contain six conserved cysteine residues that participate in the intrachain disulfide bonding required for the structural stability of the motif (38). (*f*) Also present is a 24-amino acid hydrophobic sequence C-terminally to the EGF-like domain (Iso^{1101}-Iso^{1124}) suggesting a membrane-spanning region.

Identification of the SPACRCAN Gene Product—The putative GAG attachment sites in the deduced amino acid sequence of SPACRCAN (Fig. 4) and the identification of SPACRCAN′s restricted retinal expression to photoreceptors (Fig. 3, *A* and *B*) suggest that SPACRCAN may be a candidate for a singularly abundant chondroitin sulfate proteoglycan core protein in the human IPM that was recently characterized using a ΔDi6S monoclonal antibody following digestion of the human IPM samples with chondroitinase ABC (23). To identify this 230-kDa core protein, the protein band was cut from the gel following PAGE of chondroitinase ABC-digested IPM extracts and submitted for N-terminal analysis. Accordingly, the sequence SILFP was obtained, which is identical to residues Ser^{82}-Pro^{86} in the deduced sequence of SPACRCAN (Fig. 4). Two internal peptides liberated following trypsin digestion of the 230-kDa core protein were also analyzed producing the sequences TF-WDR and VSPFLPDASMEK. These correspond to sequences Thr^{123}-Arg^{127} and Val^{582}-Lys^{593}, respectively, in the deduced sequence (Fig. 4). Thus, the 100% concordance of the amino acid sequences of these three peptides to the sequences deduced from human SPACRCAN cDNA indicates that the 230-kDa IPM chondroitin sulfate proteoglycan core protein characterized previously (23) represents the gene product of the SPACRCAN gene.

Further Carbohydrate Analysis of SPACRCAN—Insoluble IPM extracts containing SPACRCAN were analyzed with 5% SDS-PAGE before and after chondroitinase ABC digestion and stained with Gel Code Blue or the lectin wheat germ agglutinin to estimate the change in SPACRCAN mass (Fig. 5*A*). In the undigested sample, SPACRCAN migrated as a broad smear with a peak intensity close to 400 kDa (Fig. 5*A*, *lanes 1* and *3*). This apparent molecular mass was estimated using chondroitinase-digested rat chondrosarcoma aggrecan (400 kDa) as the standard (39) (Fig. 5*A*, *lane 5*). After digestion SPACRCAN was visible at a lower position at around 230 kDa, and the broad smear, present in the higher molecular weight range of the undigested sample, was absent (Fig. 5*A*, *lanes 2* and *4*).

When the IPM samples were separated using a 7.5% gel, the high molecular weight components present in the undigested IPM sample only minimally entered the gel and were present at the top of the lane as seen in the Gel Code Blue-stained gels (Fig. 5*B*, *lane 1*). Following digestion with chondroitinase ABC (Fig. 5*B*, *lane 2*), the high molecular mass band at the top of the lane was no longer present, and a new band was observed just above the 220-kDa marker. This dramatic increase in electrophoretic mobility of the high molecular weight IPM protein following chondroitinase digestions clearly indicates that this molecule represents the core protein of a chondroitin-type proteoglycan.

We also used the ΔDi6S antibody (40, 41) to label SPACRCAN in the IPM. In the Western blot using the ΔDi6S antibody (Fig. 5*B*, *lanes 3–4*), no immunostaining was evident in the undigested sample (*lane 3*), whereas intense immunostaining of the 230-kDa SPACRCAN band was present in the chondroitinase ABC-digested sample (*lane 4*). Lower levels of

[3] E. A. Turley and J. K. K. Choe, personal communication.

```
MIMFLLFGKI SLGILIFVLI EGDFPSLTAQ TYLSIEEIQE PKSAVSFLLP   50
EESTDLSLAT KKKQPLDRRE TEROWLTRRR RSILFPNGVK ICPDESVAEA  100
VANHVKYFKV RVCQEAVWEA FRTFWDRLPG REEYHYWMNL CEDGVTSIFE  150
MGTNFSESVE HRSLIMKKLT YAKETVSSSE LSSPVPVGDT STLGDTTLSV  200
PHPEVDAYEG ASESSLERPE ESISNEIENV IEEATKPAGE QIAEFSIHLL  250
GKQYREELQD SSSFHHQHLE EEFISEVENA FTGLPGYKEI RVLEFRSPKE  300
NDSGVDVYYA VTFNGEAISN TTWDLISLHS NKVENHGLVE LDDKPTVVYT  350
ISNFRDYIAE TLQQNFLLGN SSLNPDPDSL QLINVRGVLR HQTEDLVWNT  400
QSSSLQATPS SILDNTFQAA WPSADESITS SIPPLDFSSG PPSATGRELW  450
SESPLGDLVS THKLAFPSKM GLSSSPEVLE VSSLTLHSVT PAVLQTGLPV  500
ASEERTSGSH LVEDGLANVE ESEDFLSIDS LPSSSFTQPV PKETIPSMED  550
SDVSLTSSPY LTSSIPFGLD SLTSKVKDQL KVSPFLPDAS MEKELIFDGG  600
LGSGSGGQKVD LITWPWSETS SEKSAEPLSK PWLEDDDSIL PAETEDKKLV  650
LVDKMDSTDQ ISKHSKYVHD DRSIHFPEEE PLSGPAVPIF ADTAAESASL  700
TLPKHISEVP GVDDYSVTKA PLILTSVAIS ASTDKSDQAD AILREDMEQI  750
TESSNYEWFD SEVSMVKPDM QTLWTILPES ERVWTRTSSL EKLSRDILAS  800
TPQSADRLWL SVTQSTKLPP TTISTLLEDE VIMGVQDISL ELDRIGTDYY  850
QPEQVQEQNG KVGSYVEMST SVHSTEMVSV AWPTEGGDDL SYTQTSGALV  900
VFFSLRVTNM MFSEDLFNKN SLEYKALEQR FLELLVPYLQ SNLTGFQNLE  950
ILNFRNGSIV VNSRMKFANS VPPNVNNAVY MILEDFCTTA YNTMNLAIDK 1000
YSLDVESGDE ANPCKFQACN EFSECLVNPW SGEAKCRCFP GYLSVEERPC 1050
QSLCDLQPDF CLNDGKCDIM PGHGAICRCR VGENWWYRGK HCEEFVSEPV 1100
IIGITIASVV GLLVIFSAII YFFIRTLQAH HDRSERESPF SGSSRQPDSL 1150
SSIENAVKYN PVYESHRAGC EKYEGPYPQH PFYSSASGDV IGGLSREEIR 1200
QMYESSELSR EEIQERMRVL ELYANDPEFA AFVREQQVEE V
```

FIG. 4. **SPACRCAN-predicted amino acid sequence (single-lettered code) from the cDNA shown in Fig. 1.** The *underlined* residues at the N terminus (Met^{1}-Arg^{81}) are not present in the isolated protein. Met^{1}-Iso^{20} may represent the signal peptide that targets the molecule for secretion. Glu^{20}-Arg^{81} may represent a propeptide that is cleaved following secretion. A large mucin-like domain is present near the middle of the sequence (*dotted underline*) from Thr^{393} to Thr^{835}. This mucin-like domain contains 76 serine residues and 35 threonine residues, potential sites for *O*-linked glycosylation. Six consensus sites for *N*-linked oligosaccharide attachment (***N***) are present. Two tandem EGF-like motifs are present near the C-terminus (*underlined*). The six conserved cystine residues (***C***) in each of the EGF-like domains are involved in interchain disulfide bonding required for stability of the EGF-like motif. Four serine residues (***S***) are consensus sites for glycosaminoglycan attachment. A potential hyaluronan-binding motif (*double underline*) is C-terminal to the mucin domain. A highly hydrophobic region near the C-terminus (*strike through*, Iso^{1101}-Iso^{1124}) suggests a transmembrane domain.

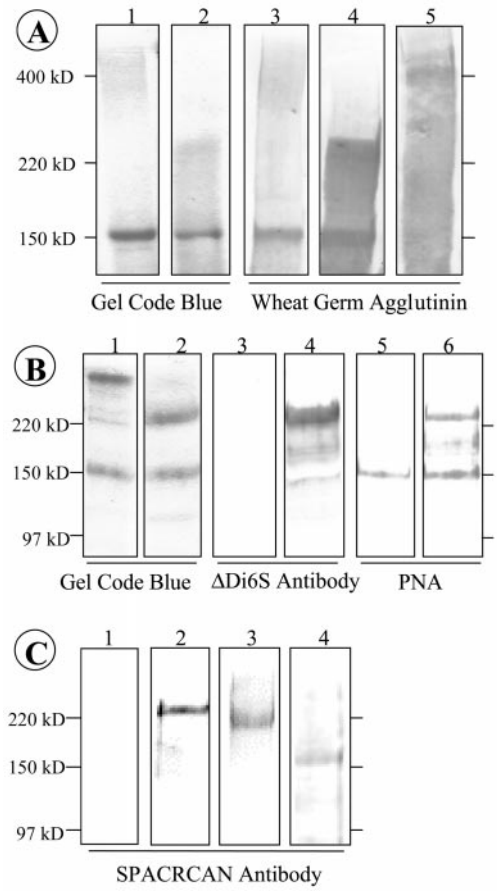

FIG. 5. *A,* IPM sample separated by gel electrophoresis using 5% acrylamide to allow the high molecular mass molecules to enter the gel. *Lanes 1* and *2* are of Gel Code Blue-stained samples. *Lanes 3–5* are wheat germ agglutinin decorated proteins electroblotted onto a transfer membrane from a 5% gel. *Lanes 1* and *3* contain undigested samples, and *lanes 2* and *4* contain samples digested with chondroitinase ABC. *Lane 5* contains a chondroitinase ABC-digested aggrecan sample to provide a molecular mass standard of approximately 400 kDa. Note the broad smear centered around the 400-kDa marker in *lanes 1* and *3*, and the movement of this component to a position just above the 230-kDa marker following chondroitinase ABC digestion in *lanes 2* and *4*. *B,* IPM sample separated by gel electrophoresis using 7.5% acrylamide. *Lanes 1* and *2* are of Gel Code Blue-stained samples. *Lanes 3* and *4* are Western blots stained with the ΔDi6S antibody. *Lanes 5* and *6* are lectin blots stained with PNA. *Lanes 1, 3*, and *5* are of the undigested sample; *lanes 2*, *4,* and *6* are of chondroitinase ABC-digested samples. Note the prominent SPACRCAN band slightly above the 220-kDa marker in *lanes 2, 4*, and *6*. *C,* IPM samples separated with 7.5% acrylamide and blotted with an anti-SACRCAN antibody. *Lane 1* is an undigested sample. *Lane 2* is a sample digested with chondroitinase ABC. Note the intense staining of SPACRCAN in *lane 2* and the absence of staining in *lane 1*. In some undigested samples, the antibody did weakly label the material that accumulates at the stacking gel, but labeling of the sample presented in *lane 1* is not evident. *Lane 3* contains a sample first digested with chondroitinase ABC followed by *N*-glycosidase digestion. *Lane 4* contains a chondroitinase ABC, *N*-, and *O*-glycosidase-digested sample. Note the progressive increase in SPACRCAN mobility following removal of the *N*- and *O*-linked carbohydrates (*lanes 2–4*).

immunoreactivity to the ΔDi6S antibody were also evident in Western blots (Fig. 5*B*, *lane 4*) in bands at approximately 170–180-kDa and 130-kDa. Absent was any immunoreactivity of the 150-kDa SPACR band, which appears devoid of any background staining (Fig. 5*B*, *lane 4*), as has recently been reported (23). In contrast, when PNA was used in lectin blotting studies, the 150-kDa SPACR band was the only region of the blot stained in the undigested IPM sample (Fig. 5*B*, *lane 5*) (21). Following chondroitinase ABC digestion, in addition to the 150-kDa SPACR band, other proteins have entered the gel, which bind PNA (Fig. 5*B*, *lane 6*). Most intensely decorated is the 230-kDa SPACRCAN band with minor labeling of bands at approximately 170–180 kDa.

The deduced sequence of SPACRCAN also contains numerous potential sites for *O*-linked sugars in the large mucin domain and six consensus sites for *N*-linked sugars (Fig. 4). To obtain direct information regarding other oligosaccharides associated with SPACRCAN we performed a series of glycosidase digestions and followed changes in electrophoretic mobility of the core protein with an anti-SPACRCAN antibody. The anti-SPACRCAN antibody was prepared using the 230-kDa band generated following chondroitinase ABC digestion. The 230-kDa band was cut from a Gel Code Blue-stained gel and used for immunizing a rabbit. Fig. 5*C*, *lanes 1* and *2* are Western blots of the crude IPM sample separated on a 7.5% SDS-PAGE gel before and after chondroitinase ABC digestion, respectively, and labeled with the anti-SPACRCAN antibody. Immunoreactivity is present only in the chondroitinase ABC-treated sample associated with the 230-kDa band (*lane 2*). No immunoreactivity is present in the undigested sample (*lane 1*), although in some preparations (not shown) weak immunoreactivity was detected at the top of the lane where SPACRCAN, with the full complement of chondroitin sulfate GAGs is presumably located. Compared with the position of chondroitinase ABC-digested SPACRCAN (Fig. 5*C*, *lane 2*), a progressive increase in mobility of SPACRCAN was observed when digested sequentially with *N*- and *O*-glycosidases (Fig. 5*C*, *lanes 3* and *4*). *N*-Glycosidase decreased the apparent molecular mass by approximately 40 kDa suggesting that *N*-linked glycoconjugates account for at least 10% of the mass of SPACRCAN. After treatment with both *N*- and *O*-glycosidases, the apparent mo-

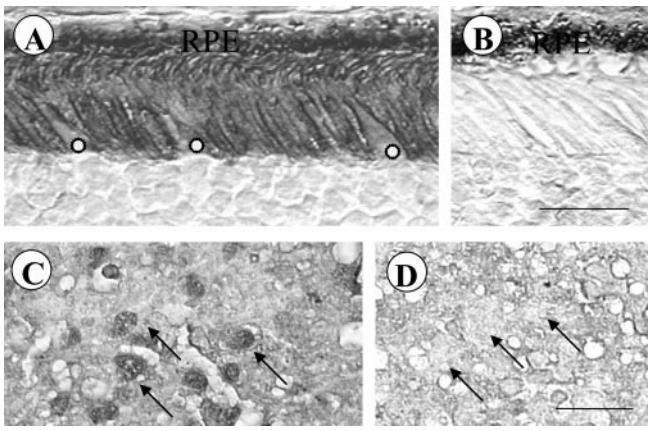

FIG. 6. **Immunocytochemistry of anti-SPACRCAN immunoreactivity in the retina from a 57-year-old male (*A* and *B*) and pineal gland from a 20-year-old male (*C* and *D*).** Tissue in *A* and *C* was incubated with the anti-SPACRCAN antibody. Tissue in *B* and *D* was incubated with preimmune serum. Note the dense immunolabeling surrounding the rod and cone photoreceptors in the IPM in *A* and the absence of labeling in *B*. The low cuboidal retinal pigment epithelium (*RPE*) contains endogenous melanin and appears as a darkly pigmented horizontal band near the *upper* border of micrographs in both immune and nonimmune-treated tissues (*A* and *B*). *Asterisks* in *A* designate cone inner segments. In the pineal gland, intense anti-SPACRCAN labeling of the pinealocytes is evident in *C* and absent in *D* (*arrows*). Adjacent experimental and control micrographs were photographed and printed at the same magnification. *Bar* in *B* and *D* represents 20 μm.

lecular mass of the remaining core protein was approximately 160 kDa. These glycosidase digestions demonstrate that SPACRCAN contains both *N*- and *O*-linked glycoconjugates, consistent with the presence of putative *N*-linked and *O*-linked glycosylation sites in the deduced sequence. Additionally, the loss of approximately 240 kDa following carbohydrate removal (from about 400 kDa in Fig. 5*A*, *lanes 1* and *3* to around 160 kDa in Fig. 5*C*, *lane 4*), suggests that glycoconjugates account for approximately 60% of the mass of SPACRCAN.

Tissue Distribution of SPACRCAN Proteoglycan—The distribution of anti-SPACRCAN immunoreactivity was established in tissue sections of human retina and pineal gland (Fig. 6). The polyclonal antibody to human SPACRCAN, which showed specific binding to the SPACRCAN band in Western blots (Fig. 5*C*, *lane 2*), also intensely labels the IPM around both rods and cones (Fig. 6*A*). In contrast, the IPM in sections treated with preimmune serum was unlabeled (Fig. 6*B*). These results indicate that in the retina, SPACRCAN is localized to the IPM where it is present around both rod and cone photoreceptors. In pineal sections, the anti-SPACRCAN antibody showed diffuse immunoreactivity with intense staining of the cell bodies of the pinealocytes, but no staining in the septal areas (Fig. 6*C*). Control sections treated with preimmune serum showed some diffuse background staining but specific pinealocyte labeling was absent (Fig. 6*D*). These data indicate that in the retina and in pineal gland, SPACRCAN is localized to the IPM, where it is present around both rod and cone photoreceptors and is present in pinealocytes, respectively. These localization patterns therefore reflect the cellular localization of SPACRCAN mRNA expression (Fig. 3).

Function of SPACRCAN—The presence of putative HA-binding motifs in the deduced amino acid sequence of SPACRCAN (Fig. 4) and the earlier reports that HA is present in the IPM (26, 42, 43) suggest that one function of SPACRCAN may be to form associative interactions with HA. To evaluate this possibility we performed experiments using CPC, a detergent that selectively precipitates GAGs and any covalently or noncovalently associated protein (44). We have demonstrated previously (21) that SPACRCAN present in IPM extracts can be selectively precipitated using CPC. This is because CPC efficiently precipitates proteoglycans through interactions with their covalently attached GAGs. When we used a hyaluronan-free preparation of SPACRCAN purified by DEAE-Sepharose ion-exchange chromatography (45) in a CPC precipitation assay, SPACRCAN was found in the pellet fraction both in the presence and absence of hyaluronan.[4] This confirms our result that the proteoglycan SPACRCAN interacts with CPC in an HA-independent manner.

To directly evaluate the binding of the core protein of SPACRCAN to HA we first digested the IPM extracts with chondroitinase ABC to remove the GAG chains, followed by PNA-agarose chromatography. Such a preparation contains mainly SPACRCAN and SPACR along with some minor PNA-binding proteins (compare Fig. 5*B*, *lanes 5* and *6*). When this sample was subjected to CPC precipitation and the pellet and supernatant components were separated with PAGE, blotted, and SPACRCAN detected with the ΔDi6S antibody, a distinct SPACRCAN band was decorated with the antibody in both the supernatant and pellet (Fig. 7, *lanes 1*). Following the addition of 50 μg/ml Healon, a source of HA, to the sample before CPC precipitation, SPACRCAN was present only in the pellet fraction (Fig. 7, *lanes 2*). However, when the sample was treated with *Streptomyces* hyaluronidase before precipitation with CPC, SPACRCAN was present only in the supernatant and not in the pellet (Fig. 7, *lanes 3*). Preincubation of the sample with HA oligosaccharides (100 μg/ml) before CPC precipitation led to the presence of SPACRCAN only in the supernatant (Fig. 7, *lanes 4*). In comparison, preincubation of the sample with HA oligosaccharides before the addition of Healon resulted in the presence of SPACRCAN in the pellet and not in the supernatant (Fig. 7, *lanes 5*). As a negative control, BSA was incubated with Healon before CPC precipitation. BSA was only present in the supernatant and not in the pellet (Fig. 7, *lanes 6*). Collectively these precipitation studies indicate that SPACRCAN can bind HA in the absence of its GAG chains.

DISCUSSION

Expression and Localization of SPACRCAN—The combined results of the Northern and *in situ* hybridization analyses indicate that SPACRCAN mRNA is present only in the retina and pineal gland and that within these multicellular tissues, SPACRCAN gene expression is restricted to rod and cone photoreceptors of the retina and pinealocytes in the pineal gland. Photoreceptors and pinealocytes are the most abundant cell type in the retina and pineal gland and these highly specialized cells are phylogenetically related (46, 47). A number of molecules expressed by retinal photoreceptors are also expressed in the pineal gland, including interphotoreceptor matrix retinoid-binding protein (48), cone arrestin (49), opsins (50), transducin (51), and several other molecules involved in the phototransduction cascade (52). SPACRCAN, initially cloned from rat pineal (24), can be added to this group of molecules that are expressed by photoreceptors and pinealocytes.

The localization pattern of SPACRCAN gene expression is also comparable to the localization of SPACRCAN protein product as demonstrated by the immunohistochemical data using the anti-SPACRCAN antibody. Furthermore, the anti-SPACRCAN antibody used in the Western blotting and immunohistochemical analyses of chondroitinase-digested human retinal tissues depicts virtually identical patterns of labeling as seen with the monoclonal ΔDi6S antibody described previously (23). These data, together with the N-terminal sequencing analysis presented in this study, demonstrate that the 230-kDa

[4] S. Acharya, V. C. Foletta, J. W. Lee, M. E. Rayborn, I. R. Rodriguez, W. S. Young III, and J. G. Hollyfield, unpublished data.

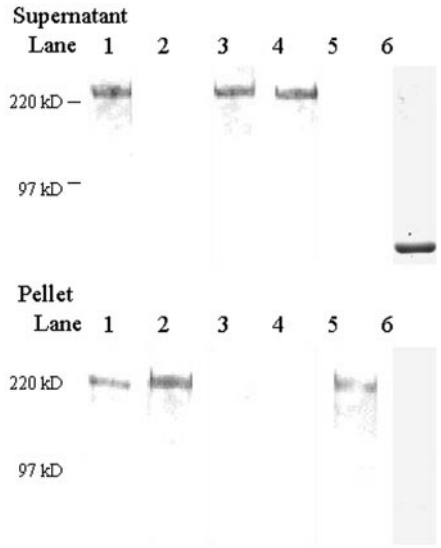

FIG. 7. **Binding of hyaluronan to SPACRCAN core protein.** The core protein of SPACRCAN was purified by PNA-agarose affinity chromatography after digestion of the IPM extract with chondroitinase ABC. Precipitation assays were performed on samples using 1.25% CPC, and both supernatant (*upper panel*) and pellets (*lower panel*) were analyzed by Western blotting using the ΔDi6S antibody after separation on 7.5% SDS-PAGE. *Lane 1* contains a PNA-purified sample precipitated with CPC. Note the immunoreactivity of SPACRCAN in both supernatant (*upper lane 1*) and pellet (*lower lane 1*), suggesting the presence of endogenous HA in the sample. *Lane 2* contains a sample preincubated with Healon (50 μg/ml) for 1 h at 37 °C before CPC precipitation. SPACRCAN is present in the pellet (*lower lane 2*) but not in the supernatant (*upper lane 2*). *Lane 3* contains purified SPACRCAN predigested with *Streptomyces* hyaluronidase for 1 h at 37 °C prior to CPC precipitation. This hyaluronidase degrades only HA, which results in the retention of SPACRCAN in the supernatant (*upper lane 3*) with none in the pellet (*lower lane 3*). *Lane 4* contains a sample preincubated with a 22-saccharide fragment of HA (100 μg/ml) for 1 h at 37 °C. This HA oligosaccharide is able to prevent CPC precipitation of SPACRCAN, as evidenced by the presence of SPACRCAN in the supernatant (*upper lane 4*) and the absence of SPACRCAN in the pellet (*lower lane 4*). The addition of Healon after preincubation of the sample with the HA oligosaccharide led to the accumulation of all SPACRCAN in the pellet only (*lower lane 5*) with none remaining in the supernatant (*upper lane 5*). *Lanes 1–5* are Western blots stained with the ΔDi6S antibody. *Lane 6* contains a Gel Code Blue-stained gel of a negative control incubation of BSA and Healon prior to CPC precipitation. Note that all BSA is retained in the supernatant (*upper lane 6*), and none is present in the pellet (*lower lane 6*).

chondroitin sulfate proteoglycan core protein is indeed SPACRCAN. It should also be noted that the retinal distribution of SPACRCAN immunoreactivity was in the IPM, an extracellular compartment, whereas in the pineal gland, these antibodies show a distribution of immunoreactivity over the pinealocytes. These fundamental differences in localization of SPACRCAN in retina and pineal gland may reflect differences in processing and/or function of this molecule in these two tissues.

Features of the Deduced Polypeptide of SPACRCAN—Because the N-terminal sequence of the SPACRCAN core protein isolated from the IPM corresponds to residues Ser^{82}-Pro^{86} in the deduced sequence, it is unlikely that residues Met^{1}-Arg^{81} are a part of the functional protein and suggests that the functional N terminus of the mature protein begins at Ser^{82}. Met^{1}-Gly^{22} is probably the signal peptide involved in the secretion of this molecule, because it has the required tripartate structure, including a central hydrophobic region (Phe^{4}-Leu^{19}) flanked by two hydrophilic sequences (Met^{1}-Met^{3} and Ile^{20}-Gly^{22}). The putative clevage site of this signal sequence conforms to the −1, −3 rule where −1 (Gly^{22}) does not have a long side chain and −3 (Ile^{20}) is not a charged amino acid (53). The remaining sequence (Asp^{23}-Arg^{81}) is likely a propeptide cleaved from the functional protein following secretion.

SPACRCAN contains two EGF-like modules near the C terminus of the deduced sequence (Fig. 4). EGF-like modules are characteristic of a number of extracellular matrix proteins and are implicated in cell-matrix interactions (54–56). Some EGF-like domains require calcium for their biological function (57). Interestingly, one of the EGF-like domains in SPACRCAN contains the critical asparagine (Asp^{1028}), which has been implicated in calcium binding (57), whereas the other domain does not. The potential for calcium binding by SPACRCAN suggests an important physiological role for this molecule in sequestering extracellular calcium released by photoreceptors in response to light (58–60).

SPACRCAN may also participate in calcium binding in the pineal through its EGF-like module. Many mammals, including humans, develop calcified inclusions with increasing age (corpora arenacea or pineal sand) (47). These inclusions consist primarily of hydroxyapatite, calcium phosphate, and an organic component (61, 62). The cause of these concretions is not known, although there are several hypotheses. They include intracellular calcium accumulation and mineralization leading to pinealocyte degeneration and subsequent release of these deposits (63), and the exchange of released polypeptides, combined with a carrier protein, for calcium by the vascular system. The calcium is then supposedly deposited as concretions (64). Whether SPACRCAN binds calcium in the pineal gland and is involved in pineal sand formation remains to be determined.

A short hydrophobic region in the deduced SPACRCAN polypeptide suggests that it could function as a membrane-spanning domain (Fig. 4, Iso^{1101}-Iso^{1124}). This region shows an average of 2.5 on the hydropathy scale, suggesting it may represent a putative membrane-spanning segment (64, 65). A similar putative transmembrane domain is also present in the predicted sequence of the rat homolog PG10.2 and other chondroitin and heparin sulfate proteoglycans, including neuroglycan C and the syndecan family (24, 66–68). It should be noted that the procedures used to isolate SPACRCAN from the IPM (Tris buffer extraction) would not be expected to remove proteins that are anchored to the plasma membrane in this manner. Either this putative membrane-spanning region is nonfunctional or SPACRCAN may be cleaved N-terminal to this transmembrane region and released to the extracellular compartment. Additional studies will be required to resolve this issue.

Hyaluronan Binding of SPACRCAN—The CPC precipitation studies indicate that SPACRCAN can bind HA in the absence of its GAG chains. The finding that CPC can partially precipitate SPACRCAN in the absence of exogenous HA suggests that endogenous HA is in the sample but not at a sufficient concentration to interact with all the SPACRCAN molecules present, because some SPACRCAN remains in the supernatant (Fig. 7, *lanes 1*). One might argue that the precipitation by CPC was due to the presence of incompletely digested chondroitin sulfate on SPACRCAN. Our finding that CPC precipitation of SPACRCAN was eliminated when the sample was digested with HA-specific hyaluronidase (Fig. 7, *lanes 3*), clearly indicates that endogenous HA is the GAG responsible for interaction with SPACRCAN in this preparation. We were also able to block CPC precipitation of SPACRCAN by pretreatment with a 22-saccharide fragment of HA (Fig. 7, *lanes 4*), suggesting that these short HA fragments compete for HA binding of SPACRCAN more efficiently than the endogenous HA. The HA oligosaccharides were not able to prevent binding when exogenous HA was added (Fig. 7, *lanes 5*), suggesting that higher

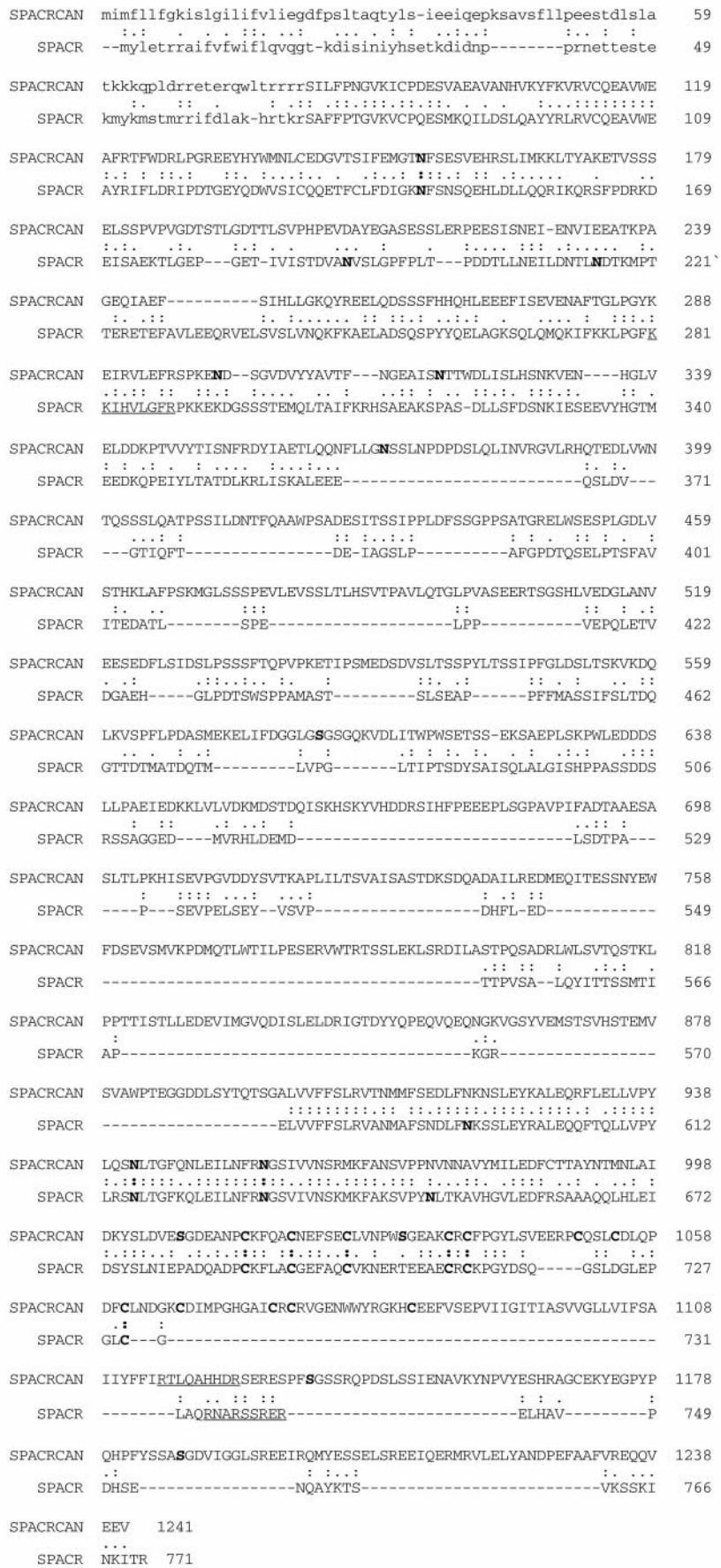

FIG. 8. **Optimal global alignment comparison of SPACRCAN and SPACR prepared with the sequence alignment utility and the FASTA algorithm available through the Munich Information Center for Protein Sequences.** *Double dots* between aligned residues indicate absolute identity; *single dots* indicate homology; *no dots* indicate no homology; and *dashes* indicate interruptions in the sequence allowing for the logical alignment of the two molecules. Asparagine residues in *bold* (***N***) represent consensus sites for *N*-linked glycosylation. Serine residues in *bold* (***S***) represent consensus sites for xylosylation and GAG attachment. The sequences beginning and ending in arginine or lysine that are *underlined* represent putative hyaluronan-binding motifs. Note that three of the consensus sites for *N*-linked glycosylation are in perfect alignment. The conserved cysteine residues in the EGF-like modules are presented in *bold* (***C***). Major regions of homology are evident over the first 350 residues of the N terminus and from SPACRCAN^{898}/SPACR^{572} to SPACRCAN^{1058}/SPACR^{727} near the C terminus.

concentrations of HA can more efficiently compete for the HA-binding sites. Collectively, these precipitation studies clearly indicate that SPACRCAN can bind HA. This function may have an important role in organization of the IPM and may be causally responsible for the difficulty in extracting this novel molecule from the IPM using physiological salt solutions. It is likely that SPACRCAN-HA interactions are mediated through the receptor for hyaluronan-mediated motility-type HA-binding motifs identified in the deduced sequence of SPACRCAN (Fig. 4) (37, 69),[3] but confirmation of these regions as binding sites must await experimental analysis.

A New Family of IPM Molecules—SPACR is another novel human IPM molecule recently characterized (20). When the deduced amino acid sequences of SPACRCAN and SPACR are aligned, several homologous regions are evident (Fig. 8). (*a*) The first 81 residues from the deduced sequence of SPACRCAN and the first 70 in SPACR are not present in the isolated molecules. From N-terminal sequence analysis we know that the functional N terminus of SPACRCAN and SPACR (20) begins at residue Ser^{81} and Ser^{71}, respectively, showing 54% homology. (*b*) The four residues immediately preceding the N-terminal sequence in both SPACRCAN (Arg^{78}-Arg^{81}) and SPACR (Arg^{67}-Arg^{70}) are rich in basic amino acids, suggesting the cleavage sites of the propeptide. (*c*) Both molecules contain a large mucin-like domain near the central portion of the sequence. (*d*) Both molecules contain clusters of *N*-linked consensus sites on either side of the mucin domains. Three of these *N*-linked sites are in perfect alignment and show 100% sequence identity. (*e*) Both molecules contain putative HA-binding motifs. (*f*) Both molecules contain EGF-like modules near the C terminus with five of the six conserved cysteine residues in precise alignment and 66% homology between these modules. SPACRCAN contains a second EGF-like domain not present in SPACR immediately downstream to the EGF-like domain described above. (*g*) Both molecules contain conserved aspartic acid/asparagine residues in their EGF domains, which are required for calcium binding. This extensive list of homologies and features shared by these two IPM molecules suggests that they represent two members of a novel family of extracellular matrix proteins.

Targets for Retinal Degeneration—The retinal- and pineal-specific expression of SPACRCAN makes this molecule a potential candidate for mutations involved in degenerative retinal and/or pineal disease. In evaluating 3q11.2 where SPACRCAN resides, no studies linking retinal or pineal diseases to this region have been reported. However, the potential involvement of SPACRCAN in degenerative retinal disease should not be dismissed *a priori* because of potentially important motifs contained in SPACRCAN. For example, the EGF-like modules are of particular interest. Recently the mutation causing Malattia Leventinese (Doyne's honeycomb retinal dystrophy), an early onset form of macular degeneration, was localized to the EFEMP1 gene. This gene codes for an extracellular matrix protein containing five EGF-like modules (70). A point mutation contained in every individual with this disorder causes an $Arg^{345} \rightarrow$ Trp conversion in the last EGF-like module of EFEMP1. Although EFEMP1 is expressed in many nonocular tissues as well as in the retina (70), this is the first documented mutation known to result in the accumulation of extracellular debris (drusen) below the retinal pigment epithelium. Drusen have been long known to be an important risk factor for age-related macular degeneration (22, 71). Drusen formation associated with a mutation in an EGF-like module in EFEMP1 suggests that mutations in other genes coding for molecules containing EGF-like modules may also be causally related to drusen formation. Novel molecules present in the outer retina, such as SPACRCAN and SPACR, which also contain EGF-like motifs, should be considered as new candidates for mutations in individuals with retinal degeneration, particularly those with late onset macular degeneration.

In conclusion, the expression analyses and binding studies of SPACRCAN demonstrate the synthesis of this novel proteoglycan by photoreceptors and pinealocytes. Considering that SPACRCAN binds HA and is the principal proteoglycan present in the human IPM, it may be of fundamental importance in organizing the IPM to support photoreceptor function in higher vertebrates.

Acknowledgments—We thank the Cleveland Eye Bank and Dr. Mary Herman of the Section of Neuropathology, Clinical Brain Disorders Branch, National Institute of Mental Health, Bethesda, MD for the human tissues used in this study. We thank Dr. Jeremy Nathans for providing the human retina cDNA library, Dr. Ivan Still for his help in identifying the expressed sequence tags used in chromosomal localization of SPACRCAN, Dr. John Hassell for his comments on potential GAG attachment sites in SPACRCAN, Dr. Eva A. Turley and John Kyu Yong Choe for their review of the deduced SPACRCAN sequence and their comments on potential HA-binding motifs, Dr. John W. Crabb for his critical review of a preprint of the manuscript, and Mrs. Karen G. Shadrach for her expert technical assistance.

REFERENCES

1. Röhlich, P. (1970) *Exp. Eye Res.* **10,** 80–96
2. Feeney, L. (1973) *Dev. Biol.* **32,** 101–114
3. Feeney, L. (1973) *Dev. Biol.* **32,** 115–128
4. Fong, S.-L., Liou, G. I., Landers, R. A., Alvarez, R. A., and Bridges, C. D. (1984) *J. Biol. Chem.* **259,** 6534–6542
5. Fong, S.-L., Liou, G. I., Landers, R. A., Alvarez, R. A., Gonzalez-Fernandez, F., Glazebrook, P. A., Lam, D. M. K., and Bridges, C. D. B. (1984) *J. Neurochem.* **42,** 1667–1676
6. Lai, Y. L., Wiggert, B., Liu, Y. P., and Chader, G. J. (1982) *Biochem. Biophys. Res. Commun.* **108,** 1601–1608
7. Hollyfield, J. G., Varner, H. H., Rayborn, M. E., and Osterfeld, A. M. (1989) in *Extracellular and Intracellular Messengers in the Vertebrate Retina* (Redburn, D. A., and Pasantes-Morales, H., eds) pp. 1–11, Alan R. Liss, Inc., New York
8. Hageman, G. S., and Johnson, L. V. (1991) *Prog. Ret. Res.* **10,** 207–249
9. Lazarus, H., and Hageman, G. (1992) *Invest. Ophthalmol. Visual Sci.* **33,** 364–376
10. Chaitin, M., Wortham, H., and Brun-Zinkeragel, A. (1994) *Exp. Eye Res.* **58,** 359–365
11. Yao, X.-Y., Hageman, G., and Marmor, M. (1990) *Invest. Ophthalmol. Visual Sci.* **31,** 2051–2058
12. Yao, X.-Y., Hageman, G., and Marmor, M. (1994) *Invest. Ophthalmol. Visual Sci.* **35,** 744–748
13. Adler, A. J., and Klucznik, K. M. (1982) *Exp. Eye Res.* **34,** 423–434
14. Adler, A. J., and Severin, K. M. (1981) *Exp. Eye Res.* **32,** 755–769
15. Berman, E. R., and Bach, G. (1968) *Biochem. J.* **108,** 75–88
16. Plantner, J. (1992) *Exp. Eye Res.* **54,** 113–125
17. Plantner, J. (1992) *Curr. Eye Res.* **11,** 91–101
18. Wood, J. G., Besharse, J. C., and Napier-Marshall, L. (1984) *J. Comp. Neurol.* **228,** 299–307
19. Porrello, K., and LaVail, M. M. (1986) *Curr. Eye Res.* **5,** 981–993
20. Acharya, S., Rayborn, M. E., and Hollyfield, J. G. (1998) *Glycobiology* **8,** 997–1006
21. Acharya, S., Rodriguez, I. R., Moreira, E. F., Midura, R. J., Misono, K., Todres, E., and Hollyfield, J. G. (1998) *J. Biol. Chem.* **273,** 31599–31606
22. Green, W. R., and Enger, C. (1993) *Ophthalmology* **100,** 1519–1535
23. Hollyfield, J., Rayborn, M., Midura, R., Shadrach, K., and Acharya, S. (1999) *Exp. Eye Res.* **69,** 311–322
24. Wang, X., Brownstein, M. J., and Young, W. S., III (1996) *Mol. Brain Res.* **41,** 269–273
25. Hollyfield, J. (1999) *Invest. Ophthalmol. Visual Sci.* **40,** 2765–2767
26. Hollyfield, J., Rayborn, M., Tammi, M., and Tammi, R. (1998) *Exp. Eye Res.* **66,** 241–248
27. Sambrook, J., Fritsch, E. F., and Maniatis, T. (1989) in *Molecular Cloning* (Nolan, C., ed) Vol. 1, pp. 7.39–7.52, Cold Spring Harbor Laboratory Press, Cold Spring Harbor, NY
28. Schoen, T. J., Mazuruk, K., Chader, G. J., and Rodriguez, I. R. (1995) *Biochem. Biophys. Res. Commun.* **213,** 181–188
29. Spiess, A., and Ivell, R. (1999) *BioTechniques* **26,** 46–48
30. Bradley, D., Towle, H., and Young, W. S., III (1994) *Proc. Natl. Acad. Sci. (U. S. A.)* **91,** 439–443
31. Hollyfield, J. G., Rayborn, M. E., and Landers, R. A. (1990) *Exp. Eye Res.* **50,** 335–338
32. Laemmli, U. K. (1970) *Nature* **227,** 680–685
33. Kozak, M. (1991) *J. Cell Biol.* **115,** 887–903
34. Hudson, T., Stein, L., Gerety, S., Ma, J., Castle, A., Silva, J., Slonim, D., Baptista, R., Kruglyak, L., and Xu, S. (1995) *Science* **22,** 1945–1954
35. Bourdon, M. A., Oldberg, A., Pierschbacher, M., and Ruoslahti, E. (1985) *Proc. Nat. Acad. Sci. U. S. A.* **82,** 1321–1325
36. Mann, D. M., Yamaguchi, Y., Bourdon, M. A., and Ruoslahti, E. (1990) *J. Biol. Chem.* **265,** 5317–5323

37. Yang, B., Yang, B., Savani, R., and Turley, E. (1994) *EMBO J.* **13,** 286–296
38. Handford, P. A., Mayhew, M., Baron, M., Winship, P. R., Campbell, I. D., and Brownlee, G. G. (1991) *Nature* **351,** 164–167
39. Plaas, A. H. K., Wong-Palms, S., Roughley, P. J., Midura, R. J., and Hascall, V. C. (1997) *J. Biol. Chem.* **272,** 20603–20610
40. Couchman, J. R., Caterson, B., Christner, J. E., and Baker, J. R. (1984) *Nature* **307,** 650
41. Shibata, S., Midura, R. J., and Hascall, V. C. (1992) *J. Biol. Chem.* **267,** 6548–6555
42. Berman, E. R. (1969) *Mod. Probl. Ophthal.* **8,** 5–31
43. Berman, E. R. (1982) *Methods Enzymol.* **81,** 77–85
44. Scott, J. E. (1973) *Biochem. Soc. Trans.* **1,** 787–806
45. Hascall, V., Calabro, A., Midura, R., and Yanagishita, M. (1994) *Methods Enzymol.* **230,** 390–417
46. Eakin, R. E. (1973) *The Third Eye*, University of California Press, Berkeley, CA
47. Arendt, J. (1995) *Melatonin and the Mammalian Pineal Gland, Structure of the Pineal*, pp. 18–23, Chapman and Hall, London
48. Rodrigues, M. M., Hackett, J., Gaskins, R., Wiggert, B., Lee, L., Redmond, M., and Chader, G. J. (1986) *Invest. Ophthalmol. Visual Sci.* **27,** 844–850
49. Craft, C. M., Whitmore, D. H., and Wiechmann, A. F. (1994) *J. Biol. Chem.* **269,** 4613–4619
50. Vigh, B., Rohlich, P., Gorcs, T., Manzano e Silva, M., Szel, A., Fejer, Z., and Vigh-Teichmann, I. (1998) *Biol. Cell* **90,** 653–659
51. Max, M. S. A., Takahashi, J. S., Margolskee, R. F., Knox, B. E. (1998) *J. Biol. Chem.* **273,** 26820–26826
52. Blackshaw, S., and Snyder, S. (1997) *J. Neurosci.* **17,** 8074–8082
53. Martoglio, B., and Dobberstein, B. (1998) *Trends Cell Biol.* **8,** 410–415
54. Scott, J. E., and Hughes, E. W. (1983) *J. Microsc.* (*Oxf.*) **129,** 209–219
55. Gray, A., Dull, T. J., and Ulrich, A. (1983) *Nature* **303,** 722–725
56. Novenberg, U., Wille, H., Wolff, J. M., Frank, R., and Rathjen, F. G. (1992) *Neuron* **8,** 849–863
57. Selander-Sunnerhagen, M., Ullner, M., Persson, E., Teleman, O., Stenflo, J., and Drakenberg, T. (1992) *J. Biol. Chem.* **267,** 19642–19649
58. Galvez, J. M. G., Puelles, L., and Prada, C. (1977) *Exp. Neurol.* **56,** 151–157
59. Gold, G. H., and Korenbrot, J. I. (1980) *Proc. Natl. Acad. Sci. U. S. A.* **77,** 5557–5561
60. Gold, G. H. (1986) *Proc. Natl. Acad. Sci. U. S. A.* **83,** 1150–1154
61. Krstic, R. (1976) *Cell Tissue Res.* **174,** 129–137
62. Japha, J., Eder, T., and Goldsmith, E. (1976) *Acta Anat.* **94,** 533–544
63. Humbert, W., and Pevet, P. (1995) *Cell Tissue Res.* **279,** 565–573
64. Lukaszyk, A., and Reiter, R. (1975) *Am. J. Anat.* **143,** 451–164
65. Kyte, J., and Doolittle, R. (1982) *J. Mol. Biol.* **157,** 105–132
66. Watanabe, E., Maeda, N., Matsui, F., Kushima, Y., Noda, M., and Oohira, A. (1995) *J. Biol. Chem.* **270,** 26876–26882
67. Yasuda, Y., Tokita, Y., Aono, S., Matsui, F., Ono, T., Sonta, S., Watanabe, E., Nakanishi, Y., and Oohira, A. (1998) *Neurosci. Res.* **32,** 313–322
68. Bernfield, M., Kokenyesi, R., Kato, M., Hinkes, M., Spring, J., Gallo, R., and Lose, E. (1992) *Annu. Rev. Cell Biol.* **8,** 365–393
69. Yang, B., Zhang, L., and Turley, E. A. (1993) *J. Biol Chem.* **268,** 8617–8623
70. Stone, E., Lotery, A., Munier, F., Héon, E., Piguet, B., Guymer, R., Vandenburgh, K., Cousin, P., Nishimura, D., E., R., Swiderski, R., Silvestri, G., Mackey, D., Hageman, G., Bird, A., Sheffield, V., and Schorderet, D. (1999) *Nat. Genet.* **22,** 199–202
71. Bressler, N. M., Bressler, S. B., and Fine, S. D. L. (1988) *Surv. Ophthalmol.* **32,** 375–412